Mevlana Tıp Bilimleri Dergisi
Mevlana Medical Sciences
eISSN:2757-976X

ARAŞTIRMA MAKALESİ/RESEARCH ARTICLE

DOI:http:/dx.doi.org/10.56752/Mevmedsci.2026.102
Mev Med Sci, 2026; 6(1): 8-18

The Role of Dynamic Breast MRI in Predicting Pathologic Response of Mass Breast Cancers with Placed Marker Prior to Neoadjuvant Chemotherapy

Neoadjuvan Kemoterapi Öncesinde Marker Yerleştirilen Kitlesel Meme Kanserlerinde Patolojik Yanıtı Öngörmede Dinamik Meme "MRG" nin Rolü

Seyma Unuvar[1], Huseyin Unuvar[2], Abdullah Enes Atas[2], Fahriye Kilinc[3], Ganime Dilek Emlik[2], Esra Hacilar[4], Murat Araz[5], Necdet Poyraz[2]

[1]Konya City Hospital, Department of Radiology, Konya, Türkiye
[2]Necmettin Erbakan University, Faculty of Medicine, Department of Radiology, Konya, Türkiye
[3]Necmettin Erbakan University, Faculty of Medicine, Department of Pathology, Konya, Türkiye
[4]Necmettin Erbakan University, Faculty of Medicine, Department of Public Health, Konya, Türkiye
[5]Necmettin Erbakan University, Faculty of Medicine, Department of Oncology, Konya, Türkiye

Makale Tarihleri/Article Dates:
Geliş Tarihi/Received: 15 November 2025
Kabul Tarihi/Accepted: 12 December 2025
Yayın Tarihi/Published Online: 10 April 2026

Sorumlu Yazar/Corresponding Author:
Seyma Unuvar
Konya City Hospital, Department of Radiology, Konya, Türkiye
e mail: seymababaoglu@hotmail.com

Açıklama/Disclosure: Yazarların hiçbiri, bu makalede bahsedilen herhangi bir ürün, aygıt veya ilaç ile ilgili maddi çıkar ilişkisine sahip değildir. Araştırma, herhangi bir dış organizasyon tarafından desteklenmedi. Yazarlar çalışmanın birincil verilerine tam erişim izni vermek ve derginin talep ettiği takdirde verileri incelemesine izin vermeyi kabul etmektedirler.

ÖZET

Amaç: Bu çalışma, dinamik meme Manyetik Rezonans Görüntüleme (MRG)' nin marker yerleştirilmiş lokal ileri meme kanserlerinde neoadjuvan kemoterapi (NAKT) sonrası, patolojik tam yanıtı (pTY) öngörebilme yeteneğini araştırmış olup MRG bulgularını altın standart olan post-operatif patolojiyle karşılaştırmıştır.
Yöntemler: Ultrasonografi eşliğinde marker yerleştirilen 85 meme kitlesine sahip 71 NAKT hastasının, 2020-2023 yılları arasındaki Dinamik Kontrastlı Meme MRG incelemeleri retrospektif olarak değerlendirildi. Patoloji sonuçlarına kör iki radyolog tarafından, RECIST 1.1 kriterleri kullanılarak, MRG'de radyolojik yanıt (rY) değerlendirildi. Patolojik değerlendirmede pTY, invaziv karsinom yokluğu olarak tanımlandı. İstatistiksel analizde Kappa, sensitivite, spesifite, PPV ve NPV hesaplandı.
Bulgular: NAKT sonrası MRG'de %52,9 oranında radyolojik tam yanıt (rTY) saptanırken, patolojik olarak %45,2 oranında pTY doğrulandı. rY ile patolojik yanıt (pY) arasında güçlü uyum gözlendi ($p < 0,001$, $\kappa = 0,740$). MRG'nin tanısal performansı %80 sensitivite, %94,7 spesifite, %95 pozitif prediktif değer (PPV) ve %80 negatif prediktif değer (NPV) sağladı. Yanlış negatifler; mikroskobik tümörler, dosetaksel etkileri, artefaktlar, düşük histolojik derece ve luminal alt tip ile ilişkiliydi. Yanlış pozitifler ise HER2 pozitifliği, granülasyon ve fibrozis ile bağlantılıydı.
Sonuç: MRG, marker yerleştirilen meme kanserlerinde NAKT sonrası patolojik yanıt ile yüksek spesifite sergileyerek etkin bir şekilde korele olmaktadır. MRG ile tam yanıt elde eden hastalarda pTY, cerrahi olmaksızın vakum destekli biyopsiyle doğrulanabilir; ancak bunun için daha büyük ve uzun dönem çalışmalara ihtiyaç vardır.

Anahtar Kelimeler: Manyetik rezonans görüntüleme, neoadjuvan kemoterapi, marker, radyolojik yanıt, patoloji, meme kanseri

ABSTRACT

Objective: This study investigated the ability of dynamic breast magnetic resonance imaging (MRI) to predict pathological complete response (pCR) after neoadjuvant chemotherapy (NACT) in locally advanced breast cancer with marker placement and compared MRI findings with the gold standard postoperative pathology.
Methods: We retrospectively evaluated Dynamic Contrast-Enhanced MRI exams of 85 breast masses in 71 NACT patients with ultrasonography-guided marker placement (2020-2023). Two radiologists, blinded to pathology, assessed the radiologic treatment response (rR) on MRI using RECIST 1.1. Pathological evaluation defined pCR as absence of invasive carcinoma. Statistical analysis provided Kappa, sensitivity, specificity, PPV, and NPV.
Results: Post-NACT MRI showed 52.9% radiological complete response (rCR), while pathology confirmed 45.2% pCR. Strong concordance between rR and pathological response (pR) was observed ($p < 0.001$, $\kappa = 0.740$). MRI's diagnostic performance yielded 80% sensitivity, 94.7% specificity, 95% positive predictive value (PPV) and 80% negative predictive value (NPV). False negatives related to microscopic tumors, docetaxel effects, artifacts, low histological grade, and luminal subtype. False positives linked to HER2 positivity, granulation, and fibrosis.
Conclusion: MRI effectively correlates with pR post-NACT in marker-placed breast cancers, showing high specificity. For patients with MRI-evaluated complete response, pCR might be confirmed non-surgically by vacuum-assisted biopsy, though larger, long-term studies are needed for validation.

Key words: Magnetic resonance imaging, neoadjuvant chemotherapy, marker, radiologic response, pathology, breast cancer

Atıf yapmak için/ Cite this article as: Unuvar S, Unuvar H, Atas AE, Kilinc F, Emlik GD, Hacilar E, Araz M, Poyraz N. The Role of Dynamic Breast Mri in Predicting Pathologic Response of Mass Breast Cancers with Placed Marker Prior To Neoadjuvant Chemotherapy. Mev Med Sci. 2026; 6(1): 8-18

INTRODUCTION

Breast cancer, the most common neoplasm in women, accounts for 31% of all cancers. Its incidence rises annually, with decreasing age at diagnosis. Due to prevalence among younger women and cosmetic concerns, breast-conserving surgery (BCS) has gained importance (1,2). Over half of early-onset breast carcinoma patients (under 40-50 years) are diagnosed at locally advanced stages (3). Neoadjuvant chemotherapy (NACT) is standard for locally advanced breast cancers, improving survival in stage I-III cases (3). Recent advances led to novel targeted therapies integrated into chemotherapy (CT) (4). NACT aims to reduce recurrence in non-metastatic breast cancer, offering benefits like disease downstaging, increased BCS feasibility, reduced mortality and morbidity through limited axillary dissection, and prognostic information for adjuvant CT. Contemporary agents increased pathological complete response (pCR) rates after NACT. Primary breast lesions respond to NACT in 80–90% of cases, complicating tumor localization and pathological evaluation (5). Placing a marker within the mass enables accurate localization and favorable cosmetic outcomes. Without pre-treatment marking, tumor bed delineation is challenging, forcing surgeons to choose between BCS and unnecessary mastectomies. Preoperative tumor localization is now standard for NACT patients (6). Radiodense markers are most effective for identifying the tumor bed among various methods. Markers are visualized through ultrasonography (US) and mammography (MG), then wire-localized under stereotactic guidance (1).

Dynamic Contrast-Enhanced Magnetic Resonance Imaging (DCE-MRI) is the standard imaging method for assessing treatment response before and after NACT in locally advanced breast cancer. Radiological complete response (rCR) is defined as absence of visible enhancement at the initial tumor site or enhancement equal to or less than background parenchymal enhancement (7) (Figure 1). Post-NACT MRI shows high sensitivity and specificity in assessing treatment response, detecting residual tumors to guide surgery, predict CT response, potentially preventing treatment-related adverse effects (8). Pathological complete response (pCR) is defined as absence of residual invasive carcinoma in the tumor bed, lymph nodes, and intravascular tumor cells (9). pCR is a strong predictor of long-term survival. The definitive NACT response is determined by post-operative pathology. Kataoka et al. (2023) showed absence of residual tumor at the marker site after NACT accurately predicts pCR (10). Currently, surgery remains standard even with pCR after NACT. Due to surgery's invasive nature and cosmetic impact, alternative treatments are investigated. MRI response prediction after NACT may be crucial for patient selection.

This study investigates the role of dynamic breast MRI in evaluating the outcomes of NACT by correlating postoperative histopathological findings with MRI results. Specifically, we focused on patients with pre-treatment mass lesions, evaluating whether the absence of residual tumor on post-NACT MRI corresponds to pCR in surgical specimens. The aim of this study is to determine the accuracy of MRI in detecting pCR in the tumor bed following NACT.

MATERIALS AND METHODS

Patient Population

DCE-MRI examinations of patients with marker placement in breast masses prior to NACT at our university's breast unit (November 2020–August 2023) were retrospectively evaluated. The study included 85 masses in 71 patients who received NACT and underwent surgery. Eleven patients had multiple masses, evaluated separately. Patients with non-mass enhancement were excluded as unsuitable for marker placement. Of 122 patients with marker placement, 51 were excluded due to unavailable pathology/MRI data (n=35), treatment refusal/death (n=6), and no surgery (n=10) (Figure 2).

NACT eligibility, marker placement, and surgical procedures were determined by a multidisciplinary breast tumor board. Marker placement was performed under US-guidance before NACT. Gold tumor markers (GEOTEK®) or silver wires were used based on patient selection. Marker number was determined by tumor characteristics, agreed by 2 radiologists. Small lesions received one central marker; larger ones got peripheral markers. The marker was located by US before surgery and wire-marked. Specimen mammography confirmed marker excision during surgery.

Neoadjuvant Chemotherapy Protocol

NACT regimens included anthracyclines, alkylating agents, taxanes, and platinum agents by subtype. HER2-positive and triple-negative patients received doxorubicin-cyclophosphamide followed by paclitaxel cycles, with carboplatin in select cases. HER2-positive patients received doxorubicin-cyclophosphamide, then docetaxel with trastuzumab and pertuzumab. Post-NACT MRI was done one week after chemotherapy. Surgery was planned three weeks after NACT.

MRI Protocol and Evaluation

MRI examinations used a dedicated breast coil on a 1.5-Tesla Siemens Symphony system in prone position. Sequences included T2-weighted fat-suppressed (T2W FS), T1W turbo spin-echo (TSE) non-FS axial, diffusion-weighted imaging (DWI), and DCE FS sequences. Gadolinium-based contrast (gadoteric acid, 0.1 mmol/kg) was administered intravenously at 3 ml/s, with six axial dynamic series at 30-second intervals. Imaging parameters were: T2W (slice thickness (st) 5 mm, TR 5880 ms, TE 55 ms, matrix 240×320);

pre-contrast T1W non-FS (st 5 mm, TR 601 ms, TE 10 ms, matrix 240×320); post-contrast T1W (TE 1.59 ms, TR 4.24 ms, matrix 240×320); DWI (st 5 mm, FOV 320 mm, matrix 132×174). Two radiologists with 12 and 4 years breast imaging experience independently reviewed MRI images, blinded to post-operative pathology results. In cases of disagreement between the two initial readers, a consensus was reached following the consultation of a third radiologist with 20 years breast imaging experience. Reporting followed American College of Radiology Breast Imaging Reporting and Data System 5th edition guidelines, evaluating all baseline dynamic breast MRI sequences, DWI, and post-NACT MRIs. Fibroglandular tissue was categorized on pre-contrast non-FS T1W images as fatty, scattered, heterogeneous, or dense fibroglandular. T1W and T2W sequences assessed ductal and nipple-skin findings, lesions, structural distortion, artifacts, and lymphadenopathy. Dynamic post-contrast early phase images evaluated background parenchymal enhancement.

For baseline mass lesions, shape, margins, internal enhancement patterns, laterality, and multiplicity were recorded. Lesion size was measured on delayed-phase dynamic images. Additional findings were documented. Treatment response was evaluated using RECIST 1.1. Complete response meant absence of enhancing lesions in the primary tumor bed on post-NACT MRI. Partial response, stable and progressive disease were classified per RECIST 1.1 as non-complete radiological responses (non-rCR).

Pathological Evaluation

Baseline tru-cut biopsy and post-operative pathology reports were retrieved for marker-placed lesions after NACT. Core biopsies from primary masses were histopathologically assessed, with carcinoma subtypes reported by classification. The Nottingham system evaluated tubular formation, nuclear pleomorphism, and mitotic activity; scores 3-5 indicated well-differentiated, 6-7 moderately, and 8-9 poorly differentiated carcinomas. Specimens were sectioned at 5-10 mm intervals. Tumor location and wire-marked site were identified by palpation, focusing tissue sampling on the marker area. Samples underwent processing, embedding, and 4 μm sectioning. H&E staining was followed by IHC staining (P63 and CK5/6) for suspicious areas. Pan-CK assessed epithelial cells. Absence of invasive carcinoma indicated pCR; presence, non-pCR. NACT effects were recorded. ER, PR, and Ki-67 index reported as percentage of positive nuclei. HER2 status was assessed by IHC (0/1+ negative, 3+ positive). Cases scoring 2+ underwent FISH testing, HER2 amplification defined as >6 signals per nucleus.

Statistical Analysis

Data analyses used SPSS 21.0, with results as mean ± SD, median (IQR), and frequencies. Normality was tested via histograms and Kolmogorov-Smirnov test. Mann-Whitney U test compared independent groups; Wilcoxon test for paired non-normal data. McNemar and McNemar-Bowker tests analyzed paired categorical data, while Chi-square and Fisher's exact tests compared independent groups. Bonferroni correction was used for post-hoc analyses. Cohen's Kappa assessed diagnostic agreement. Sensitivity, specificity, positive predictive value (PPV), and negative predictive value (NPV) were calculated. Significance was $p < 0.05$.

RESULTS

Seventy-one female patients underwent breast marker placement (November 2020–August 2023), with eleven having multiple lesions (85 total). Mean age was 50.44 ± 11.53 years (26–73). Thirty-nine patients were premenopausal and 46 postmenopausal. Lesions were distributed between right (43) and left (42) breasts. Surgeries included: total mastectomy (7), modified radical mastectomy (6), partial mastectomy (61), and subcutaneous mastectomy (10). Diagnosis MRI showed fibroglandular tissue was fatty (6 patients), dense (6), scattered (40), and heterogeneous (33). Background enhancement was minimal in 47 lesions (55.3%), mild in 18 (21.2%), moderate in 8 (9.4%), and marked in 12 (14.1%). Median lesion size was 26.5 mm (IQR: 20.0–41.0). Lesions had irregular (50.6%) or spiculated (49.4%) non-circumscribed margins. Enhancement was heterogeneous in 51 (60%), homogeneous in 27 (31.8%), and rim in 7 (8.2%). Most lesions showed diffusion restriction (97.7%) and ipsilateral axillary lymphadenopathy (71.8%).

Post-NACT MRI, mean residual lesion size was 13.67 ± 12.45 mm (3–69 mm). Median lesion size at diagnosis was significantly greater than post-NACT MRI ($p<0.001$). Internal enhancement patterns differed significantly between diagnosis and post-NACT MRI ($p = 0.012$) in non-pCR patients (Table 1). Post-NACT, 81.2% of lesions (n=69) showed no lymphadenopathy; 18.8% (n=16) remained positive. Axillary involvement decreased from 71.8% to 18.8% ($p <0.001$). Diffusion restriction on MRI decreased from 97.7% to 14.2% ($p <0.001$) (Table 2). Tru-cut biopsy showed 93% (n=79) were invasive carcinoma NST (Non-Specific Type); 7.1% (n=6) were specific subtypes. Immunohistochemistry revealed ER positivity in 64%, PR in 45%, HER2 in 43% of lesions. Molecular classification identified 54 luminal, 10 HER2-enriched, 20 triple-negative lesions. The Ki-67 index decreased from 30.0 at biopsy to 10.0 post-operatively ($p <0.001$) (Table 3). ER, PR, and HER2 statuses between biopsy and post-operative pathology showed no significant differences.

On post-NACT MRI, using RECIST 1.1, 45 lesions (53%) showed complete response; 34 (40%) partial response; 5 (5.9%) stable; and 1 (1.2%) progressive disease. Thus, 45 lesions (52.9%) were rCR; 40 (47.1%) non-rCR. Post-operative pathology showed 38 lesions (45.2%) achieved pCR; 46 lesions

Table 1. Evaluation of the internal enhancement pattern of the lesion on MRI before and after NACT using the Mc Nemar Bowker test

		Internal enhancement post- NACT				p
		Homogeneous	Heterogeneous	Rim	Total	
MRI internal contrast enhancement	Homogenus	11	0	0	11 (%37,9)*	0,012
	Heterogeneous	8	6	1	15 (%51,8)	
	Rim	2	0	1	3(%10,3)	
	Total	21 (%72,5)	6(%20,6)	2 (%6,9)	29 (%100,0)	

MRI: Magnetic Resonance Imaging, NACT: Neoadjuvant Chemotherapy

Table 2. Comparison of diffusion restriction/axillary involvement in diagnosis and post-NACT MRI using McNemar test

		Post-NACT DWI			
		No restriction	Restriction	Total	
Diagnosis DWI	No restriction	2	0	2 (%2,3)	<0.001*
	Restriction	71	12	83 (%97,7)	
	Total	73 (%85,8)	12 (%14,2)	85(%100,0)	
		Post-NACT MRI Axilla			
		Negative	Positive	Total	
MRI Axilla	Negative	23	1	24 (%28,2)	<0.001*
	Positive	46	15	61 (%71,8)	
	Total	69 (%81,2)	16 (%18,8)	85 (%100,0)	

DWI: Diffusion-Weighted Imaging, MRI: Magnetic Resonance Imaging, NACT: Neoadjuvant Chemotherapy

Table 3. Comparison of the biopsy-post-op KI67 index.

	Median (1st-3rd Quartile)	P
Biopsy pathology Ki-67	30,0 (15,0-31,3)	<0,001*
Post-operative pathology Ki-67	10,0 (5,0-25,0)	

The Wilcoxon test was used

Table 4. Radiological-pathological response correlation

Post-operative pathology				p	Kappa(κ)
		Complete response	Non-complete response		
Radiological response	Complete response	36 (%80,0)	9 (%20,0)	<0,001*	0,740
	Non-complete response	2 (%5,1)	37 (%94,9)		

(54.8%) were non-pCR. A statistically significant and strong concordance was demonstrated between radiological and pathological response (rR, pR) using the Kappa test ($p < 0.001$, $\kappa = 0.740$) (Table 4). In our study, pathological evaluation was accepted as the gold standard. The presence of invasive cells was classified as non-pCR (positive). True positives were cases where non-pCR was confirmed as non-rCR (37 lesions). False positives (n=2) were cases assessed as non-rCR but proven pCR on pathology. True negative cases (n=36) were cases with rCR and pCR. False negatives (n=9) were lesions demonstrating non-pCR but categorized as rCR.

Sensitivity was calculated as true positives (n=37) among all non-pCR cases (n=46). Specificity was true-negatives (n=36) among all pCR cases (n=38). NPV was calculated as true negatives/total negatives ×100, and PPV as true positives/total positives ×100. Diagnostic performance values were: sensitivity 80%, specificity 94.7%, PPV 95%, and NPV 80%.

Premenopausal patients showed higher rCR (66.7%, $p = 0.034$). Irregular margins correlated with higher rCR (67.4%, $p = 0.013$). No axillary MRI and diffusion restriction indicated non-rCR ($p < 0.001$) (Table 5). rR and pR correlated with PR positivity ($p = 0.012$ and 0.006), showing higher rCR in PR-negative cases (65.2%) and non-pCR in PR-positive cases (73%). No associations existed with histopathological subtype, ER/HER2 status, or post-operative ER/PR/HER2 positivity. rR and pR differed significantly from biopsy Ki-67 values (p

Table 5. Relationship between radiological response and age, laterality, mastectomy type, and MRI findings.

Radiological response				□²	p
		Complete response (%)	Non-complete response (%)		
Age	Premenopausal	26 (%66,7)	13 (%33,3)	4,47	0,034*
	Postmenopausal	19 (%41,3)	27 (%58,7)		
Laterality	Right	23 (%53,5)	20 (%46,5)	0,10	0,919
	Left	22 (%52,4)	20 (%47,6)		
Number of masses	Single	32 (%52,5)	29 (%47,5)	0,020	0,887
	Multiple	13 (%54,2)	11 (%45,8)		
Type of mastectomy	Total-radical-simple	0 (%0,0)	7 (%100,0)	11,672	0,021
	Modified radical	3(%50,0)	36(%59,0)		
	Parsiyel, segmental, BCS	6(%60,0)	25(%41,0)		
	Subcutaneous	3(%50,0)	4(%40,0)		
MRI contour	Irregular	29 (%67,4)	14 (%32,6)	6,21	0,013*
	Spicule	16 (%38,1)	26 (%61,9)		
MRI axilla	Negative	8 (%33,3)	16 (%66,7)	4,12	0,042*
	Positive	37 (%60,7)	24 (%39,3)		
Diagnosis Diffusion MRI	No restrictions	2 (%100,0)	0 (%0,0)	0,40	0,496
	Restriction	43 (%51,8)	40 (%48,2)		
Post-NACT Diffusion MRI	No restriction	45 (%61,6)	28 (%38,4)	13,34	<0,001*
	Restriction	0 (%0,0)	12 (%100,0)		
MRI fibroglandular (fg) tissue type	Almost entirely fat	3 (%50,0)	3 (%50,0)		
	Scattered fg	22 (%55,0)	18 (%45,0)	0,816	0,871
	Heterogeneous fg	16 (%48,5)	17 (%51,5)		
	Extreme fg	2 (%33,3)	4 (%66,7)		
MRI background parenchymal enhancement	Minimal	26 (%55,3)	21 (%44,7)		
	Mild	4 (%22,2)	14 (%77,8)	12,450	0,007*
	Moderate	5 (%62,5)	3 (%37,5)		
	Marked	10 (%83,3)	2 (%16,7)		
MRI internal enhancement characteristics	Homogeneous	10 (%37,0)	17 (%63,0)		
	Heterogeneous	32 (%62,7)	19 (%37,3)	4,995	0,077
	Rim	3 (%42,9)	4 (%57,1)		

BCS: Breast-Conserving Surgery, fg: Fibroglandular, MRI: Magnetic Resonance Imaging, NACT: Neoadjuvant Chemotherapy. Chi-square test was used

Table 6. Comparison of diffusion restriction/axillary involvement in diagnosis and post-NACT MRI using McNemar test

	Biopsy Median Ki-67 (1st-3rd quarter)	p	Post-operative Median Ki-67 (1st-3rd quarter)	p	Size on MRI Median (1st-3rd quarter)	p
rCR	40,0 (30,0-70,0)	<0,001*	7,5 (3,5-26,3)	0,580	28,0 (21,0-35,0)	0,791
Non-rCR	30,0 (11,3-30,0)		10,0 (5,0-25,0)		26,0 (20,0-41,0)	

MRI: Magnetic Resonance Imaging, rCR: Radiological Complete Response

<0.001 and p = 0.002), with higher Ki-67 in rCR and pCR (Table 6). pR was compared with patient age, lesion features, mastectomy type, MRI findings, and axillary involvement. MRI lesion margins showed significant difference (p = 0.027) with pR, spiculated margins having higher non-pCR (68.3%). Post-NACT DWI findings were significant (p = 0.002), with all diffusion restriction lesions showing non-pCR. Other groups showed no differences.

False-negative cases (n=9) showed common features such as invasive carcinoma (NST) with non-circumscribed contour, diffusion restriction, and loss of restriction post-NACT. All had segmental mastectomy. Six lesions were left-sided, three right. Enhancement was heterogeneous in five, homogeneous in four. Fibroglandular tissue was scattered in four, heterogeneous in four, dense in one. Molecular subtypes included one HER2-enriched, two triple-negative, two

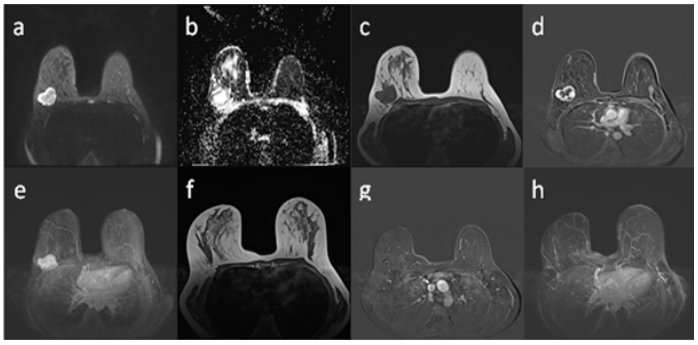

Figure 1. DCE-MRI images of a radiologically and pathologically concordant patient. MRI sections before (a,b,c,d,e) and after (f,g,h) NACT are shown for a 44-year-old patient diagnosed with triple-negative invasive carcinoma, NST. Intense diffusion restriction is observed at the periphery of the mass (a,b). The mass described in the non-FS T1W sequence appears irregular shape and contours. On the early arterial subtracted image (d) and MIP image (e), the peripherally enhancing area of the centrally necrotic mass is evident. In the post-NACT MRI, no mass is observed in the primary site on the non-FS T1W sequence (f). Absence of enhancement in the mass site on the early arterial subtracted image (g) and MIP image (h) is consistent with a rCR. In the patient's post-operative pathological evaluation, the absence of invasive tumor cells was interpreted as a pCR.

DCE-MRI: Dynamic Contrast-Enhanced Magnetic Resonance Imaging, FS: Fat-Suppressed, MRI: Magnetic Resonance Imaging, MIP: Maximum Intensity Projection, NACT: Neoadjuvant Chemotherapy, NST: Non-Specific Type, pCR: pathological complete response, rCR: Radiological Complete Response, W: Weighted

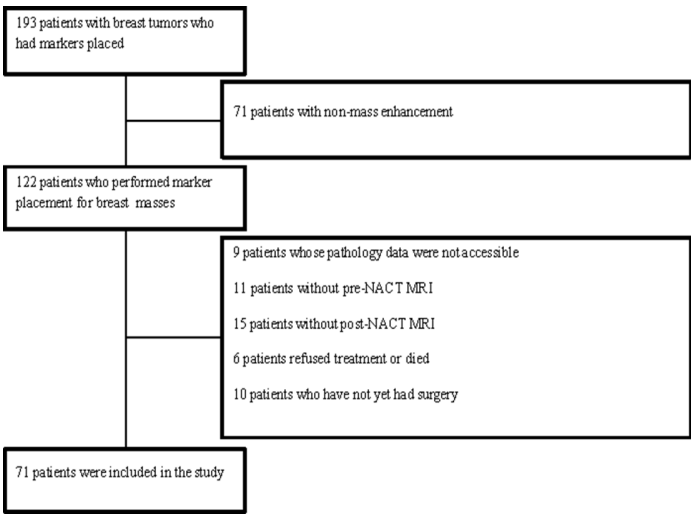

Figure 2. Flow chart

MRI: Magnetic Resonance Imaging, NACT: Neoadjuvant Chemotherapy

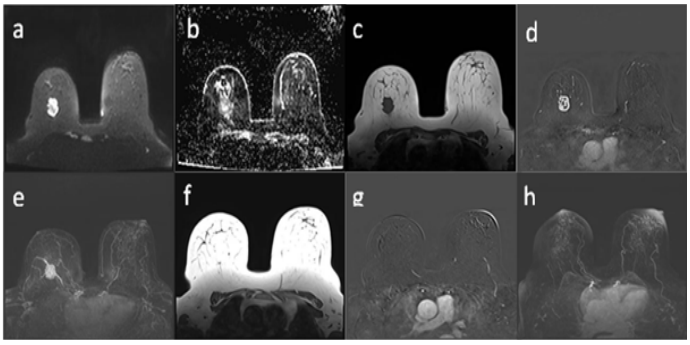

Figure 3. MRI of the radiologic-pathologic discordant patient. MRI axial dynamic breast sections at the time of diagnosis (a,b,c,d,e) and post-NACT follow-up (f,g,h) are shown for a 43-year-old female patient diagnosed with invasive carcinoma, NST, after tru-cut biopsy of the breast mass. In DWI (a,b), in the right breast, there is evidence of diffusion restriction. The mass appears irregularly shaped and contoured on the T1W non-FS sequence (c). On the post-contrast early arterial subtracted image, the mass shows heterogeneous enhancement (d). On post-NACT MRI, the mass has completely disappeared on the T1W non-FS sequence (f). On the post-contrast subtracted (g) and MIP images (h), no contrast uptake is observed in the primary mass area, consistent with a rCR.

DWI: Diffusion-Weighted Imaging, FS: Fat-Suppressed, MRI: Magnetic Resonance Imaging, MIP: Maximum Intensity Projection, NACT: Neoadjuvant Chemotherapy, NST: Non-Specific Type, rCR: Radiological Complete Reesponse, W: Weighted

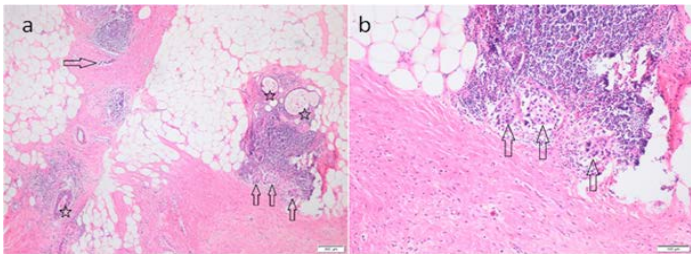

Figure 4. Microscopic sections of a patient with radiologic-pathologic discordance. Although the patient appeared to have a rCR, the pathological evaluation determined a non-pCR. Scattered and small clusters of tumor cell groups (arrows) are observed within the fibroadipose breast stroma. In other areas, benign breast ducts (stars), some of which show mild cystic dilation, and lymphocytic inflammatory cell aggregates in the stroma can be seen (a) (Hematoxylin/Eosin, 40x magnification). In the lower left corner of the breast stroma, stromal areas containing fibroblastic cells and collagen are present. The arrows indicate several small groups of tumor cells. A lymphocytic inflammatory cell reaction can be seen in the vicinity of the tumor cells (Hematoxylin/Eosin, 100x magnification) (b).

pCR: pathological complete response, rCR: Radiological Complete Response

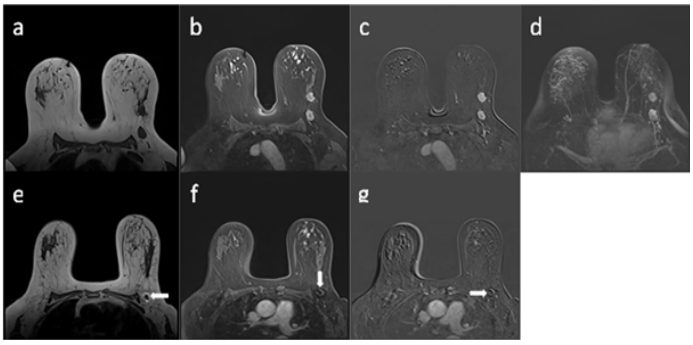

Figure 5. MRI of a false negative case. Baseline and post-NACT DCE-MRI are shown for a patient in whom a malignant lesion was detected in the left breast following a palpable mass complaint. In the FS T1W axial image of the 62-year-old female patient, an irregularly shaped, spiculated-contoured, 22 mm mass lesion is observed in the upper outer quadrant of the left breast (a). Posteriorly, a 25 mm axillary lymphadenopathy is seen. The lesion demonstrates heterogeneous enhancement in the early arterial phase (b), axial subtracted (c), and MIP images (d). In the post-NACT MRI (16 weeks later), no mass is observed in the primary tumor bed on the FS T1W sequence (e). Posteriorly, an artifact belonging to the metallic marker placed in the axillary lymphadenopathy is observed (white arrows). The absence of an enhancing lesion in the tumor and axillary lymphadenopathy bed in the early arterial (f) and subtracted (g) post-contrast images is consistent with a rCR. However, since tumor cells were detected in the pathological evaluation, it was interpreted as a non-pCR.

DCE-MRI: Dynamic Contrast-Enhanced Magnetic Resonance Imaging, FS: Fat-Suppressed, MRI: Magnetic Resonance Imaging, MIP: Maximum Intensity Projection, NACT: Neoadjuvant Chemotherapy, NST: Non-Specific Type, pCR: pathological complete response, rCR: Radiological Complete Response, W: Weighted

luminal B, and four luminal A, with grades 1 (two), 2 (five), and 3 (two) (Figure 3-4).

DISCUSSION

Locally advanced breast cancer, inoperable without distant metastasis, sees NACT as standard treatment, increasing pCR rates and reducing mortality (11,12). NACT reduces tumor size for BCS, improving cosmetics (13). Previously, such cases required post-mastectomy radiotherapy. NACT now enables BCS (37–82% rates) (14,15). Our study showed avoiding total mastectomy in 84.2% of cases. pR was divided into complete and non-complete. pCR was absence of invasive tumor focus in post-operative specimens, excluding DCIS presence as it doesn't affect prognosis (12). After NACT, 45.2% pCR, 54.8% non-pCR. In non-pCR cases, tumor size decreased in 87%, remained same in 5 patients, increased in 1. Most showed

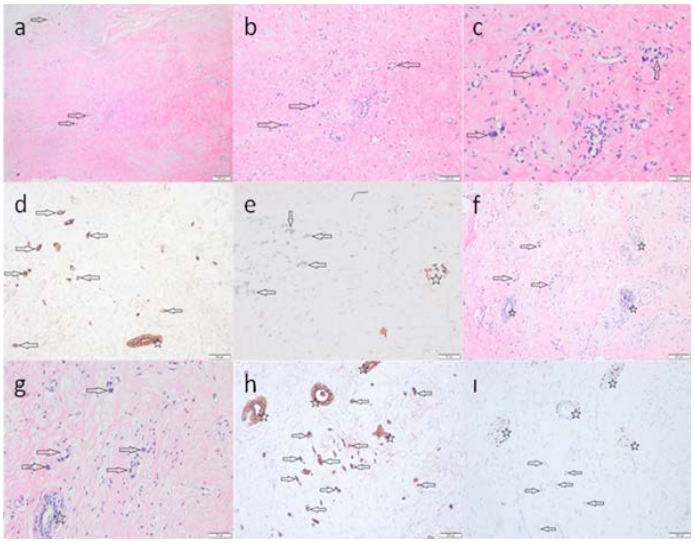

Figure 6. Pathological microscopic images of the false negative case. At low magnification, tumor cells (arrows) scattered individually or in small groups and dilated small-caliber vascular structures are seen in fibrotic breast stroma (Hematoxylin/Eosin, 40x magnification) (a). In the fibrotic breast stroma, dilated small-caliber vessels and tumor cells (arrows) scattered individually or in groups are visible (b) (Hematoxylin/Eosin, 100x magnification). Close-up view (c); in fibrotic breast stroma, dilated small-caliber vessels, lymphocytes, and tumor cells (arrows) scattered individually or in groups are observed (Hematoxylin/Eosin, 200x magnification). Immunohistochemically, with Pankeratin, tumor cells scattered individually or in groups show immunoreactivity (arrows), with a benign breast duct (star) below (d) (Pankeratin, 100x magnification). With P63, tumor cells (arrows) are immunonegative without myoepithelial cell layer. A benign breast duct (star) with P63 positive myoepithelial cells is seen (P63, 200x magnification) (e). In fibrotic breast stroma, between benign ducts (star), tumor cells (arrows) scattered individually or in groups are present (f) (Hematoxylin/Eosin, 100x magnification). In fibrotic stroma, lymphocytes, small vessels, a benign duct (star), and tumor cells (arrows) scattered individually or in groups are visible (g) (Hematoxylin/Eosin, 200x magnification). With Pankeratin, tumor cells showing cytoplasmic positivity (arrows) are seen as invasive cells. Benign ducts marked with star (Pankeratin, 100x magnification) (h). With P63, nuclear immunoreactivity is seen in myoepithelial cells of benign ducts (stars), while invasive tumor cells in groups are immunonegative (arrows) (P63, 100x magnification) (ı)

treatment response. Studies show improved response rates with CT regimen developments (16). 1990s anthracycline studies showed 10-15% pCR, Popa found 17.1% (17, 18). Adding taxanes nearly doubled pCR (19). Heil's 2015 study showed 56.7% pCR, higher in HER2-positive and triple-negative (20). Our NACT protocol used anthracyclines, alkylating agents, taxanes, and platinum-group chemotherapeutics based on patient and receptor status. With 10 HER2-positive, 20 triple-negative, and 54 hormone receptor positive patients, our overall pCR rate (45.2%) is lower than current literature. Molecular subtypes differ in NACT response. PR-positive patients had higher non-pCR (73%, $p = 0.006$). PR-negative patients showed higher rCR (65.2%). Studies show pathological response varies by subtype (16). pCR rates are lower in hormone receptor–positive/HER2-negative (8.3%), reaching 18.7% with hormone receptor and HER2 positivity, 31.1% in triple-negative, and 38.9% when HER2 is positive and hormone receptors are negative (12). No significant relationship was found between HER2 status and rR/pR, possibly due to insufficient biopsy results relative to total patients.

As pCR rates rose, tumor-free surgeries increased, and tumor size decreased significantly. Non-surgical treatment after NACT in breast cancer is increasingly explored. Post-surgery, 5% of patients develop wound infection; 45% experience pain, movement issues, and psychological disorders (21). CT alone would reduce morbidity and improve cosmetics. Studies aim to determine pR without surgery in patients with complete response after NACT, using breast core biopsy, fine-needle biopsy, local excision, and vacuum biopsy, comparing survival and recurrence rates in long-term follow-up. Mauriac et al.'s 1999 study showed 33% clinical complete response in NACT patients receiving radiotherapy (RT). After 124 months, local recurrence was 34% in RT versus 22.5% in mastectomy patients (22). Ring et al.'s study compared RT-only with post-surgery RT patients, finding no significant survival difference at 10 years, though local recurrence varied (21%/10%). Salvage surgery prevented further recurrence (23). Daveau et al. found no significant survival differences between groups (24). Clouth et al.'s study using RT alone for clinical-radiological complete response showed 12.5% recurrence in non-surgical versus 10.6% in surgical groups, though punch biopsy sampling may have been inadequate (15).

Placing tumor bed markers before NACT could improve pR assessment. Clinical evaluation alone cannot determine non-surgical treatment after NACT, with residual tumor detection rates of 53-75%. Earlier non-standardized protocols prevented accurate pR prediction, risking increased recurrence. For post-NACT treatment without surgery, pR must be accurately predicted through imaging. NCCN recommends repeating pre-NACT imaging and multidisciplinary decisions. Digital mammography predicts pCR with 75% accuracy, exceeding physical examination (19). Mammography accuracy decreases with undetectable tumors or microcalcifications. Calcifications may change after NACT and occur in necrosis, though MG best detects microcalcifications before and after NACT (26). US surpasses physical examination and MG for post-NACT evaluation (79-82% accuracy in predicting residual disease) (19). MRI enables objective tumor assessment and accurately predicts pCR. DCE-MRI is most reliable for evaluating NACT response (25), providing tumor microvascular patterns through contrast distribution, while US and MG only show tumor size (27). In our study, rCR was defined as enhancement equal to or less than fibroglandular tissue in the primary tumor bed after NACT. MRI evaluated 52.9% of lesions as rCR, 47.1% as non-rCR. Agreement between rR and pR was statistically significant ($p < 0.001$, $\kappa = 0.740$). MRI's diagnostic performance yielded 80% sensitivity, 94.7% specificity, 95% PPV, and 80% NPV. Literature MRI sensitivity ranges between 50-97%, specificity 25-100%, NPV 47-73%, and PPV 71-100% (27).

Among 38 pCR patients, MRI indicated complete response in 36, yielding 94.7% specificity. In two pCR patients, contrast enhancement was detected in the tumor bed, and MRI was misinterpreted. False positivity in literature includes granulation tissue with vascularity secondary to NACT, sclerosis–necrosis replacing tumor, DCIS component with invasive component, and HER2 overexpression. HER2-positive cancers show pronounced vascularity, high proliferation, and respond well to NACT. In HER2-positive patients, residual angiogenesis may appear on MRI after NACT without tumor. MRI diagnostic performance decreases in the HER2-enriched subtype. Careful evaluation should be performed in patients with this molecular subtype on post-NACT MRI (27, 28). Kim et al. 2022 recommended faint residual enhancement seen only in late phase be evaluated as rCR (29). In our study, one of two false-positive patients had HER2-enriched subtype, likely causing residual angiogenesis. Therefore, we may have interpreted pseudo-enhancement as residual disease on MRI. In the other patient, granulation tissue and residue may not have been distinguishable.

Of 46 non-pCR lesions, MRI detected residue in 37 (80% sensitivity). However, nine lesions were complete response on MRI, but invasive carcinoma was pathologically (Figure 5-6). MRI is insufficient in detecting diffuse microscopic invasive tumor foci and scattered tumor cells in necrotic tissue areas (30, 31). In five of nine false-negative lesions, with no mass or non-mass enhancement on MRI, sparse scattered tumor cells were observed microscopically. Literature suggests docetaxel's anti-vascular effect may suppress inflammatory response around tumor cells, leading to non-enhancing areas on MRI

(27). In our study, docetaxel in NACT protocols for three patients with radiological–pathological discordance possibly caused their MRI evaluation as complete response. In four with rCR, metallic marker artifact diameter on post-NACT MRI was larger than other marker artifacts. Retrospectively, marker types placed in the tumor bed were not standardized due to procurement differences. Metallic markers in these four caused more artifacts and hypointense areas on MRI than other types. Therefore, in these four lesions, enhancement from residual tumor could not be observed. MRI marker appearance varies with metal type, magnetic field strength (1.5–3 Tesla), and sequence. SE and gradient-echo sequences differ in metal sensitivity. In gradient-echo sequences, metallic artifact size increases compared to spin-echo sequences. The metallic artifact appears as a hypointensity larger than the marker, or as a hyperintense halo around it. A marker with good US visibility, low migration, clear MRI visualization, and minimal artifact is preferred. Matthias et al. (2022) suggested marker presence and types may affect MRI diagnostic accuracy. However, no significant difference was found in diagnostic performance between marker presence and the two types evaluated (25). In triple-negative breast cancer, MRI's NPV is higher than in luminal-type breast cancer (32). Triple-negative breast cancer shows the highest specificity (27). In our study, 67% of nine patients with radiological–pathological discordance had luminal-type breast cancer on post-operative evaluation, which may explain the discordance (one HER2 positive, two triple-negative, two luminal B, and four luminal A). Choi et al.'s (2019) study found low histological grade was associated with false negativity (33). For histological grade characteristics in our study, 7 of the 9 false-negative lesions were grade 1 (n = 2) and grade 2 (n = 5), while 2 were grade 3. Most (77.8%) of the nine false-negative lesions having a low histological grade may explain the radiological–pathological discordance. Another study examining radiological–pathological discordance in MRI, the rCR rate was 37.5% (pCR 40.2%), and non-mass enhancement and multicentricity were associated with discordance (27). Previous studies found microcalcifications on pre-NACT MG, multifocality/multicentricity, non-mass enhancement, ER positivity, and low nuclear grade associated with radiological–pathological discordance (33–35). As our study excluded US/MG findings and non-mass MRI enhancements, microcalcification and non-mass enhancement cannot explain radiology–pathology discordance.

After NACT, radiological evaluation is difficult due to varying degrees of necrosis, fibrosis, and fragmentation. Imaging's sensitivity and specificity are insufficient to assess pR and make treatment decisions without surgery and radiotherapy (32). MRI shows tumor size after NACT but cannot replace surgical excision in evaluating pR. To capture residual disease missed by MRI, studies confirm pR through multiple biopsies from the marker bed. Vacuum-assisted biopsy shows superiority over fine-needle and core biopsies, with 94.4% NPV vs. 70% with other methods (20). Kataoka et al.'s (2023) study stated pCR can be detected accurately by evaluating the marker-placed tumor bed area (10). Therefore, in patients with MRI-evaluated complete response, pCR may be detected without surgery using vacuum-assisted biopsy from the marker bed. However, these studies need larger patient populations for validation. Our study has limitations. As a single-center retrospective study, patient sample size was small. We defined pCR, regardless of DCIS presence. Non-mass enhancement was excluded from the MRI. Markers used could not be standardized due to retrospective design. Only MRI was assessed, excluding MG and US findings. Axillary status was not considered. Quantitative dynamic MRI analyses were not conducted.

We evaluated radiology-pathology correlation using MRI after NACT in patients with locally advanced breast cancer with markers. MRI assessment showed 80% sensitivity, 94.7% specificity, 95% PPV, and 80% NPV. False negatives were attributed to microscopic tumor cells, insufficient enhancement after docetaxel, metallic artifact variability, low histological grade, and luminal subtype cancer. False positives were linked to HER2 positivity, granulation tissue, and fibrosis. For patients with rCR on MRI, biopsy confirmation can detect residual microscopic tumors. We suggest patients with pCR confirmed by vacuum biopsy may be followed without surgery. To validate this approach and ensure reliable clinical adoption, future studies involving dynamic contrast-enhanced MRI and vacuum biopsy with long-term follow-up must demonstrate a higher Negative Predictive Value (above 80%). For vacuum-assisted biopsy to be a true alternative to surgery, large-scale validation studies must not only increase patient numbers but also implement methodological standardization of the number of biopsies taken from the marker bed and the sampling protocols.

Ethics Committee Approval: This study was conducted with the ethical approval of the Necmettin Erbakan University Non-Pharmaceutical and Non-Medical Device Research Ethics Committee, dated September 15, 2023, and numbered 2023/4544.

Conflict of interest: The authors declared no conflicts of interest with respect to the authorship and/or publication of this article.

Financial conflict of interest: Author declares that he did not receive any financial support in this study.

Address correspondence to: Şeyma Ünüvar,
Konya City Hospital, Department of Radiology, Konya, Türkiye
e-mail: seymababaoglu@hotmail.com

REFERENCES

1. Rüland AM, Hagemann F, Reinisch M, et al. Using a New Marker Clip System in Breast Cancer: Tumark Vision® Clip- Feasibility Testing in Everyday Clinical Practice. Breast Care. 2018;13(2):116–20.
2. Kanyılmaz G, Aktan M, Yavuz BB et al. Meme Kanserinde 5 Yıllık Tedavi Sonuçlarımız ve Prognostik Faktörler: Tek Merkez Deneyimi. Selçuk tıp Dergisi. 2017;33(1):5–9.
3. Whitman GJ, Iyer RB, Reeve CJ, et al. Assessment of response to neoadjuvant chemotherapy in breast cancer: Imaging considerations. Semin Breast Dis. 2004;7(2):61–74.
4. Soliman AH, Osman AM. Cost-effectiveness of ultrasound-guided surgical clips placement for breast cancer localization prior to neoadjuvant chemotherapy. Egyptian Journal of Radiology and Nuclear Medicine [Internet]. 2018;49(4):1163–8. Available from: https://doi.org/10.1016/j.ejrnm.2018.06.010
5. Youn I, Choi SH, Kook SH, et al. Ultrasonography-guided surgical clip placement for tumor localization in patients undergoing neoadjuvant chemotherapy for breast cancer. J Breast Cancer. 2015;18(1):44–9.
6. Hossam A, El-Badrawy A, Khater A, et al. The Evaluation of a Cost-Effective Method for Tumour Marking Prior to Neo-Adjuvant Chemotherapy Using Silver Rods. Eur J Breast Health. 2023;19(1):99–105.
7. Zhang X, Wang D, Liu Z, et al. The diagnostic accuracy of magnetic resonance imaging in predicting pathologic complete response after neoadjuvant chemotherapy in patients with different molecular subtypes of breast cancer. Quant Imaging Med Surg. 2020;10(1):197–210.
8. Romeo V, Accardo G, Perillo T, et al. Assessment and prediction of response to neoadjuvant chemotherapy in breast cancer: A comparison of imaging modalities and future perspectives. Cancers (Basel). 2021;13(14):1–18.
9. Amin MB, Edge SB, Greene FL, et al. AJCC cancer staging manual. Vol. 1024. Springer; 2017.
10. Kataoka A, Sawaki M, Horisawa N, et al. The Absence of Cancer in the Location of a Breast Tissue Marker After Neoadjuvant Chemotherapy may Predict Pathological Complete Response with High Accuracy: Results from a Phase II Trial. Ann Surg Oncol [Internet]. 2023;30(6):3224–32. Available from: https://doi.org/10.1245/s10434-023-13199-8
11. Aebi S, Karlsson P, Wapnir IL. Locally advanced breast cancer. Breast [Internet]. 2022;62: S58–62. Available from: https://doi.org/10.1016/j.breast.2021.12.011
12. Parra RFD Van, Kuerer HM. Selective elimination of breast cancer surgery in exceptional responders: Historical perspective and current trials. Breast Cancer Research [Internet]. 2016;1–8. Available from: http://dx.doi.org/10.1186/s13058-016-0684-6
13. Shalaby LASED, Khallaf ES el din, Moussa MM. Clip and wire localization of locally advanced malignant breast masses in patients undergoing neoadjuvant chemotherapy and breast conservation therapy. Egyptian Journal of Radiology and Nuclear Medicine. 2019;50(1).
14. Mitzi IIM, Freire G, Carrara A, Scapulatempo-neto IC, Lucas II, Abraha F, et al. Breast-conserving surgery in locally advanced breast cancer submitted to neoadjuvant chemotherapy. Safety and effectiveness based on ipsilateral breast tumor recurrence and long-term follow-up. 2017;134–42.
15. Clouth B, Chandrasekharan S, Inwang R, et al. The surgical management of patients who achieve a complete pathological response after primary chemotherapy for locally advanced breast cancer. 2007; 33:961–6.
16. Sanli AN, Turan B, Tekcan Sanli DE, et al. Neoadjuvant response stratification based on complete, partial, and no response in HR-positive/HER2-positive breast cancer. Breast Cancer Res Treat [Internet]. 2025;(August). Available from: https://doi.org/10.1007/s10549-025-07812-5
17. Popa E, Croitoru A, Cristian D, et al. Surgical features after neoadjuvant treatment for breast cancer. Chirurgia (Romania). 2021;116(2):193–200.
18. Wolmark N, Wang J, Mamounas E, et al. Preoperative Chemotherapy in Patients With Operable Breast Cancer: Nine-Year Results From National Surgical Adjuvant Breast and Bowel Project B-18 AND. 2001;15212(30).
19. Wong SM, Santos JDL, Basik M. Eliminating Surgery in Early-Stage Breast Cancer: Pipe-Dream or Worthy Consideration in Selected Patients? 2017;148–55.
20. Heil J, Ku S, Schaefgen B, et al. Diagnosis of pathological complete response to neoadjuvant chemotherapy in breast cancer by minimal invasive biopsy techniques. 2015;(October):1565–70.
21. Noordaa MEM Van Der, Duijnhoven FH Van, Loo CE, et al. Identifying pathologic complete response of the breast after neoadjuvant systemic therapy with ultrasound guided biopsy to eventually omit surgery: Study design and feasibility of the MICRA trial (<u>M</u>inimally <u>I</u>nvasive <u>C</u>omplete <u>R</u>e. The Breast. 2018;
22. Mauriac L, Macgrogan G, Avril A, et al. Original article Neoadjuvant chemotherapy for operable breast carcinoma larger than 3 cm: A unicentre randomized trial with a 124-month median follow-up. 1999;47–52.
23. Ring BA, Webb A, Ashley S, et al. Following Neoadjuvant Chemotherapy for Early Breast Cancer? 2015;21(24):4540–5.
24. Aveau CAD, Avignoni ALS, Oumya S, Nane AB, Endale MID, Ranc F, et al. Is Radiotherapy an option for early breast cancers with complete clinical response after neoadjuvant chemotherapy? ois campana, M. D., * Patients characteristics. 2011;79(5):1452–9.
25. Matthias H, Clémence B, Electra S, et al. Diagnostic precision of breast MRI in prediction of pathological complete response: Is it influenced by the presence of metallic markers? Eur J Radiol. 2022;154(July).
26. Talec H, Aubé C, Guerin-Charbonnel C, et al. The use of a clip prior to neoadjuvant chemotherapy for breast cancer with microcalcifications may not always be required. Breast Cancer Res Treat [Internet]. 2025;209(3):585–93. Available from: https://doi.org/10.1007/s10549-024-07517-1
27. Kwon M ri, Chu J, Kook SH, et al. Factors associated with radiologic-pathologic discordance in magnetic resonance imaging after neoadjuvant chemotherapy for breast cancer. Clin Imaging [Internet]. 2022;89(April):1–9. Available from: https://doi.org/10.1016/j.clinimag.2022.05.002
28. Moon H, Han W, Lee JW, et al. Age and HER2 expression status affect MRI accuracy in predicting residual tumor extent after neo-adjuvant systemic treatment. 2009;(January):636–41.
29. Kim J, Han BK, Ko EY, et al. Prediction of pathologic complete response on MRI in patients with breast cancer receiving neoadjuvant chemotherapy according to molecular subtypes. Eur Radiol [Internet]. 2022;32(6):4056–66. Available from: https://doi.org/10.1007/s00330-021-08461-0
30. Turnbull LW. Dynamic contrast-enhanced MRI in the diagnosis and management of breast cancer. 2009;(March 2008):28–39.
31. Morrow M, Waters J, Morris E. Breast Cancer 1 MRI for breast cancer screening, diagnosis, and treatment. The Lancet [Internet]. 2011;378(9805):1804–11. Available from: http://dx.doi.org/10.1016/S0140-6736(11)61350-0
32. Richter H, Hennigs A, Schaefgen B, et al. Is Breast Surgery Necessary for Breast Carcinoma in Complete Remission Following Neoadjuvant Chemotherapy? Ist eine Operation der Brust bei Komplettremission

nach neo- adjuvanter Chemotherapie des Mammakarzinoms notwendig? Authors Historical Studies on. 2018;48–53.
33. Choi WJ, Kim HH, Cha JH, et al. Complete response on MR imaging after neoadjuvant chemotherapy in breast cancer patients: Factors of radiologic-pathologic discordance. Eur J Radiol [Internet]. 2019;118(March):114–21. Available from: https://doi.org/10.1016/j.ejrad.2019.06.017
34. Ko ES, Han B kyung, Kim RB, et al. Analysis of Factors that Influence the Accuracy of Magnetic Resonance Imaging for Predicting Response after Neoadjuvant Chemotherapy in Locally Advanced Breast Cancer. 2013;2562–8.
35. Negrão EMS, Souza JA, Marques EF, et al. Breast cancer phenotype influences MRI response evaluation after neoadjuvant chemotherapy. Eur J Radiol [Internet]. 2019;120(September):108701. Available from: https://doi.org/10.1016/j.ejrad.2019.108701